

MULTI-SCALE CONTEXT AGGREGATION BY DILATED CONVOLUTIONS

Fisher Yu

Princeton University

Vladlen Koltun

Intel Labs

ABSTRACT

State-of-the-art models for semantic segmentation are based on adaptations of convolutional networks that had originally been designed for image classification. However, dense prediction and image classification are structurally different. In this work, we develop a new convolutional network module that is specifically designed for dense prediction. The presented module uses dilated convolutions to systematically aggregate multi-scale contextual information without losing resolution. The architecture is based on the fact that dilated convolutions support exponential expansion of the receptive field without loss of resolution or coverage. We show that the presented context module increases the accuracy of state-of-the-art semantic segmentation systems. In addition, we examine the adaptation of image classification networks to dense prediction and show that simplifying the adapted network can increase accuracy.

1 INTRODUCTION

Many natural problems in computer vision are instances of dense prediction. The goal is to compute a discrete or continuous label for each pixel in the image. A prominent example is semantic segmentation, which calls for classifying each pixel into one of a given set of categories (He et al., 2004; Shotton et al., 2009; Kohli et al., 2009; Krähenbühl & Koltun, 2011). Semantic segmentation is challenging because it requires combining pixel-level accuracy with multi-scale contextual reasoning (He et al., 2004; Galleguillos & Belongie, 2010).

Significant accuracy gains in semantic segmentation have recently been obtained through the use of convolutional networks (LeCun et al., 1989). Specifically, Long et al. (2015) showed that convolutional network architectures that had originally been developed for image classification can be successfully repurposed for dense prediction. These repurposed networks substantially outperform the prior state of the art on challenging semantic segmentation benchmarks. This prompts new questions motivated by the structural differences between image classification and dense prediction. Which aspects of the repurposed networks are truly necessary and which reduce accuracy when operated densely? Can dedicated modules designed specifically for dense prediction improve accuracy further?

Modern image classification networks integrate multi-scale contextual information via successive pooling and subsampling layers that reduce resolution until a global prediction is obtained (Krizhevsky et al., 2012; Simonyan & Zisserman, 2015). In contrast, dense prediction calls for multi-scale contextual reasoning in combination with full-resolution output. Recent work has studied two approaches to dealing with the conflicting demands of multi-scale reasoning and full-resolution dense prediction. One approach involves repeated up-convolutions that aim to recover lost resolution while carrying over the global perspective from downsampled layers (Noh et al., 2015; Fischer et al., 2015). This leaves open the question of whether severe intermediate downsampling was truly necessary. Another approach involves providing multiple rescaled versions of the image as input to the network and combining the predictions obtained for these multiple inputs (Farabet et al., 2013; Lin et al., 2015; Chen et al., 2015b). Again, it is not clear whether separate analysis of rescaled input images is truly necessary.

In this work, we develop a convolutional network module that aggregates multi-scale contextual information without losing resolution or analyzing rescaled images. The module can be plugged into existing architectures at any resolution. Unlike pyramid-shaped architectures carried over from image classification, the presented context module is designed specifically for dense prediction. It is a rectangular prism of convolutional layers, with no pooling or subsampling. The module is based on dilated convolutions, which support exponential expansion of the receptive field without loss of resolution or coverage.

As part of this work, we also re-examine the performance of repurposed image classification networks on semantic segmentation. The performance of the core prediction modules can be unintentionally obscured by increasingly elaborate systems that involve structured prediction, multi-column architectures, multiple training datasets, and other augmentations. We therefore examine the leading adaptations of deep image classification networks in a controlled setting and remove vestigial components that hinder dense prediction performance. The result is an initial prediction module that is both simpler and more accurate than prior adaptations.

Using the simplified prediction module, we evaluate the presented context network through controlled experiments on the Pascal VOC 2012 dataset (Everingham et al., 2010). The experiments demonstrate that plugging the context module into existing semantic segmentation architectures reliably increases their accuracy.

2 DILATED CONVOLUTIONS

Let $F, G : \mathbb{Z}^2 \rightarrow \mathbb{R}$ be two discrete functions. Let $\Omega_r = [-r, r]^2 \cap \mathbb{Z}^2$ and let $k : \Omega_r \rightarrow \mathbb{R}$ be a discrete filter of size $(2r + 1)^2$. The discrete convolution operator $*$ can be defined as

$$G(\mathbf{p}) = \sum_{\mathbf{s}+\mathbf{t}=\mathbf{p}} F(\mathbf{s}) * k(\mathbf{t}). \quad (1)$$

We now generalize this operator. Let l be a scale factor and let $*_l$ be defined as

$$G(\mathbf{p}) = \sum_{\mathbf{s}+l\mathbf{t}=\mathbf{p}} F(\mathbf{s}) *_l k(\mathbf{t}). \quad (2)$$

We will refer to $*_l$ as a dilated convolution or an l -dilated convolution. The familiar discrete convolution (1) is simply the 1-dilated convolution.

Our definition has many precursors. Most notably, the *algorithme à trous* for wavelet decomposition uses dilated filters (Holschneider et al., 1987; Shensa, 1992). We do not apply the term *algorithme à trous* to our work since the *algorithme à trous* is an algorithm for wavelet decomposition that applies a single pre-determined filter at successively larger scales to produce a signal decomposition. In contrast, our work involves large filter banks learned by backpropagation (Rumelhart et al., 1986). The input, output, and processing steps are all substantially different from the *algorithme à trous*. We also prefer to treat the dilated convolution as a distinct operator, instead of applying the standard discrete convolution with dilated filters. Our definition matches the proper implementation of the approach, which can apply a dilated convolution with any scale factor and any filter without constructing dilated filters.

In recent work on convolutional networks for semantic segmentation, Long et al. (2015) analyzed filter dilation but chose not to use it. Chen et al. (2015a) used dilation to simplify the architecture of Long et al. (2015), but did not go further and design new network architectures based on dilated convolutions. We further simplify the architecture of Chen et al. (2015a) and develop a new convolutional network structure that systematically uses dilation for multi-scale context aggregation.

Our architecture is motivated by the fact that dilated convolutions support exponentially expanding receptive fields without losing resolution or coverage. Let $F_0, F_1, \dots, F_{n-1} : \mathbb{Z}^2 \rightarrow \mathbb{R}$ be discrete functions and let $k_0, k_1, \dots, k_{n-2} : \Omega_1 \rightarrow \mathbb{R}$ be discrete 3×3 filters. Consider applying the filters with exponentially increasing dilation:

$$F_{i+1} = F_i *_i k_i \quad \text{for } i = 0, 1, \dots, n - 2. \quad (3)$$

Define the receptive field of an element \mathbf{p} in F_{i+1} as the set of elements in F_0 that modify the value of $F_{i+1}(\mathbf{p})$. Let the size of the receptive field of \mathbf{p} in F_{i+1} be the number of these elements. It is

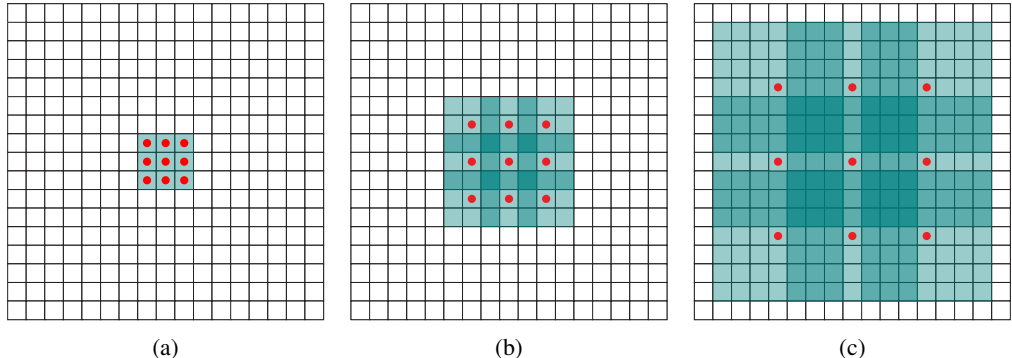


Figure 1: Systematic dilation supports exponential expansion of the receptive field without loss of resolution or coverage. (a) F_1 is produced from F_0 by a 1-dilated convolution; each element in F_1 has a receptive field of 3×3 . (b) F_2 is produced from F_1 by a 2-dilated convolution; each element in F_2 has a receptive field of 7×7 . (c) F_3 is produced from F_2 by a 4-dilated convolution; each element in F_3 has a receptive field of 15×15 . Note that the number of parameters associated with each layer is identical. The receptive field grows exponentially while the number of parameters grows linearly.

easy to see that the size of the receptive field of each element in F_{i+1} is $(2^{i+2} - 1) \times (2^{i+2} - 1)$. The receptive field is a square of exponentially increasing size. This is illustrated in Figure 1.

3 MULTI-SCALE CONTEXT AGGREGATION

The context module is designed to increase the performance of dense prediction architectures by aggregating multi-scale contextual information. The module takes C feature maps as input and produces C feature maps as output. The input and the output have the same form, thus the module can be plugged into existing dense prediction architectures.

We begin by describing a basic form of the context module. In this basic form, each layer has C channels. The representation in each layer is the same and could be used to directly obtain a dense per-class prediction, although the feature maps are not normalized and no loss is defined inside the module. Intuitively, the module can increase the accuracy of the feature maps by passing them through multiple layers that expose contextual information.

The basic context module has 7 layers that apply 3×3 convolutions with different dilations. The dilations are 1, 1, 2, 4, 8, 16, and 1 respectively. Each convolution operates on all layers: strictly speaking, these are $3 \times 3 \times C$ convolutions with dilation in the first two dimensions. Each of these convolutions is followed by a pointwise truncation $\max(\cdot, 0)$. A final layer performs $1 \times 1 \times C$ convolutions and produces the output of the module. The architecture is summarized in Table 1. Note that the front-end module that provides the input to the context network in our experiments produces feature maps at 64×64 resolution. We therefore stop the exponential expansion of the receptive field after layer 6.

Our initial attempts to train the context module failed to yield an improvement in prediction accuracy. Experiments revealed that standard initialization procedures do not readily support the training of the module. Convolutional networks are commonly initialized using samples from random distributions (Glorot & Bengio, 2010; Krizhevsky et al., 2012; Simonyan & Zisserman, 2015). However, we found that random initialization schemes were not effective for the context module. Training the context module initialized by standard random schemes did not produce filters that increased the accuracy of the input feature maps. We found an alternative initialization with clear semantics to be much more effective:

$$k^b(\mathbf{t}, a) = 1_{[\mathbf{t}=0]}1_{[a=b]}, \quad (4)$$

where a is the index of the input feature map and b is the index of the output map. This is a form of identity initialization, which has recently been advocated for recurrent networks (Le et al., 2015). This initialization sets all filters such that each layer simply passes the input directly to its successor. A natural concern is that this initialization could put the network in a mode where backpropagation cannot significantly improve the default behavior of simply passing information

Layer	1	2	3	4	5	6	7	8
Convolution	3×3	3×3	3×3	3×3	3×3	3×3	3×3	1×1
Dilation	1	1	2	4	8	16	1	1
Truncation	Yes	Yes	Yes	Yes	Yes	Yes	Yes	No
Receptive field	3×3	5×5	9×9	17×17	33×33	65×65	67×67	67×67
Output channels								
Basic	C	C	C	C	C	C	C	C
Large	$2C$	$2C$	$4C$	$8C$	$16C$	$32C$	$32C$	C

Table 1: Context network architecture. The network processes C feature maps by aggregating contextual information at progressively increasing scales without losing resolution.

through. However, experiments indicate that this is not the case: backpropagation reliably harvests the contextual information made available by the network to increase the accuracy of the processed maps.

This completes the presentation of the basic context network. Our experiments show that even this basic module can increase dense prediction accuracy both quantitatively and qualitatively. This is particularly notable given the small number of parameters in the network: $\approx 64C^2$ parameters in total.

We have also trained a larger context network that uses a larger number of feature maps in the deeper layers. The number of maps in the large network is summarized in Table 1. We generalize the initialization scheme to account for the difference in the number of feature maps in different layers. Let c_i and c_{i+1} be the number of feature maps in two consecutive layers. Assume that C divides both c_i and c_{i+1} . The initialization is

$$k^b(\mathbf{t}, a) = \begin{cases} \frac{C}{c_{i+1}} & \mathbf{t} = 0 \text{ and } \left\lfloor \frac{aC}{c_i} \right\rfloor = \left\lfloor \frac{bC}{c_{i+1}} \right\rfloor \\ \varepsilon & \text{otherwise.} \end{cases} \quad (5)$$

Here $\varepsilon \sim \mathcal{N}(0, \sigma^2)$ and $\sigma \ll C/c_{i+1}$. The use of random noise breaks ties among feature maps with a common predecessor.

4 FRONT END

We implemented and trained a front-end prediction module that takes a color image as input and produces $C = 21$ feature maps as output. The front-end module follows the work of Long et al. (2015) and Chen et al. (2015a), but was implemented separately. We adapted the VGG-16 network (Simonyan & Zisserman, 2015) for dense prediction and removed the last two pooling and striding layers. Specifically, each of these pooling and striding layers was removed and convolutions in all subsequent layers were dilated by a factor of 2 for each pooling layer that was ablated. Thus convolutions in the final layers, which follow both ablated pooling layers, are dilated by a factor of 4. This enables initialization with the parameters of the original classification network, but produces higher-resolution output. The front-end module takes padded 512×512 images as input and produces feature maps at resolution 64×64. We use reflection padding: the buffer zone is filled by reflecting the image about each edge.

Our front-end module is obtained by removing vestiges of the classification network that are counter-productive for dense prediction. Most significantly, we remove the last two pooling and striding layers entirely, whereas Long et al. kept them and Chen et al. replaced striding by dilation but kept the pooling layers. We found that simplifying the network by removing the pooling layers made it more accurate. We also remove the padding of the intermediate feature maps. Intermediate padding was used in the original classification network, but is neither necessary nor justified in dense prediction.

We now evaluate the simplified prediction module versus the FCN-8s design of Long et al. (2015) and the DeepLab network of Chen et al. (2015a). To focus on the accuracy of the basic prediction modules, we only use Pascal VOC 2012 images for training. Our module is trained on the VOC-2012 training set, augmented by annotations from Hariharan et al. (2011). We did not use images

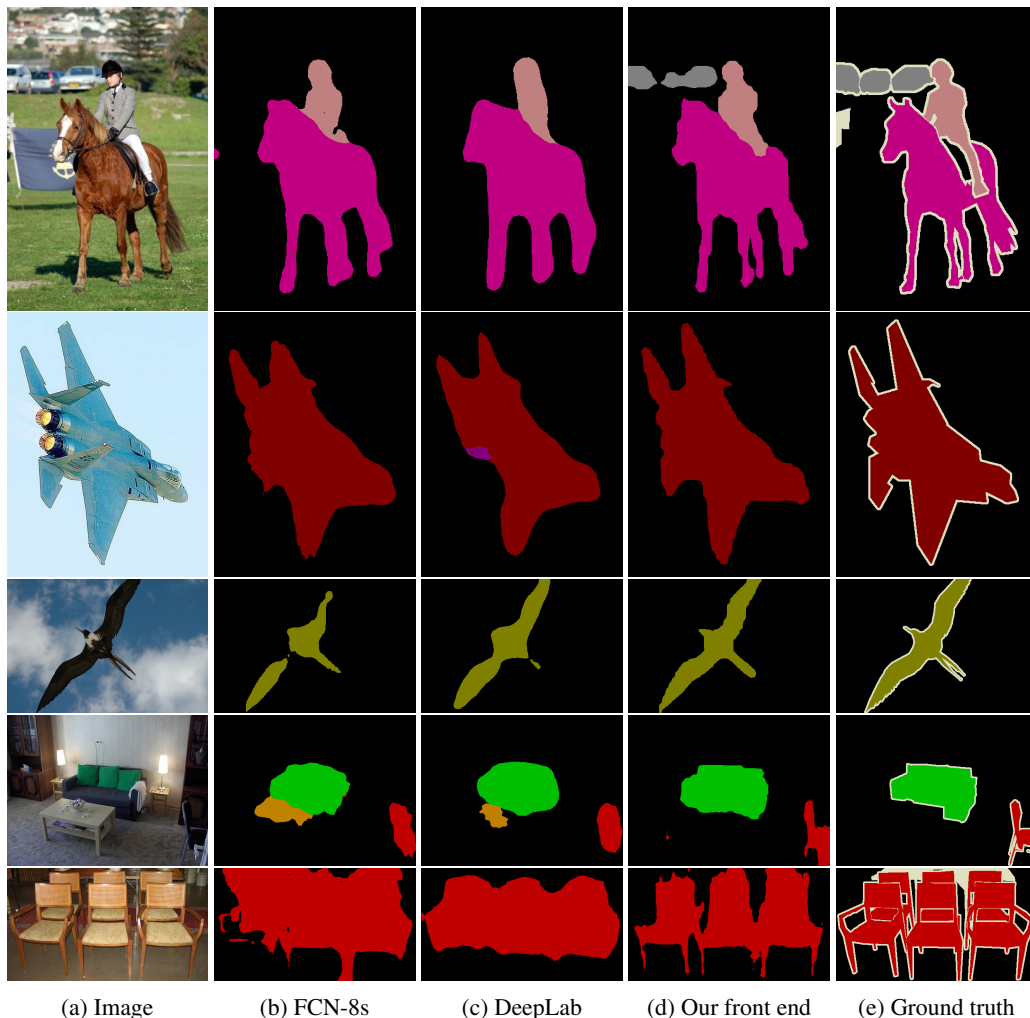


Figure 2: Semantic segmentations produced by different adaptations of the VGG-16 classification network. From left to right: (a) input image, (b) prediction by FCN-8s (Long et al., 2015), (c) prediction by DeepLab (Chen et al., 2015a), (d) prediction by our simplified front-end module, (e) ground truth.

	areo	bike	bird	boat	bottle	bus	car	cat	chair	cow	table	dog	horse	mbike	person	plant	sheep	sofa	train	tv	mean IoU
FCN-8s	76.8	34.2	68.9	49.4	60.3	75.3	74.7	77.6	21.4	62.5	46.8	71.8	63.9	76.5	73.9	45.2	72.4	37.4	70.9	55.1	62.2
DeepLab	72	31	71.2	53.7	60.5	77	71.9	73.1	25.2	62.6	49.1	68.7	63.3	73.9	73.6	50.8	72.3	42.1	67.9	52.6	62.1
Our front end	82.2	37.4	72.7	57.1	62.7	82.8	77.8	78.9	28	70	51.6	73.1	72.8	81.5	79.1	56.6	77.1	49.9	75.3	60.9	67.6

Table 2: Our front-end prediction module is both simpler and more accurate than prior models. This table reports accuracy on the VOC-2012 test set.

from the VOC-2012 validation set for training and therefore only used a subset of the annotations created by Hariharan et al. (2011). For FCN-8s and DeepLab, we evaluate the public models trained by the original authors on VOC-2012. The accuracy of these models on the VOC-2012 test set is reported in Table 2. Qualitative results are shown in Figure 2.

Our front-end prediction module is both simpler and more accurate than the prior models. Specifically, our simplified model outperforms both FCN-8s and the DeepLab network by more than 5 percentage points on the test set. Interestingly, our simplified front-end module outperforms the leaderboard accuracy of DeepLab+CRF on the test set by more than a percentage point (67.6% vs. 66.4%) without using a CRF.

5 EXPERIMENTS

Our implementation is based on the Caffe library (Jia et al., 2014). To implement dilated convolutions, we modified the `im2col` and `col2im` functions in Caffe.

For fair comparison with recent high-performing systems, we trained a front-end module that has the same structure as described in Section 4, but is trained on additional images from the Microsoft COCO dataset (Lin et al., 2014). We used all images in Microsoft COCO with at least one object from the VOC-2012 categories. Annotated objects from other categories were treated as background. The training is performed in two stages. First, we train on images from VOC-2012 and Microsoft COCO together. The learning rate is set to 10^{-3} and momentum is set to 0.9. Next, we fine-tune on VOC-2012 images alone. Since the annotations in Microsoft COCO are less precise, fine-tuning on VOC data increases prediction accuracy. For this fine-tuning stage, the learning rate is set to 10^{-5} . We again do not use images from the validation set for training. The front-end module trained by this procedure achieves 69.8% mean IoU on the VOC-2012 validation set and 71.3% mean IoU on the test set. Note that this level of accuracy is achieved by the front-end alone, without the context module or structured prediction. We again attribute this high accuracy in part to the removal of vestigial components originally developed for image classification rather than dense prediction.

Controlled evaluation of context aggregation. We now perform controlled experiments to evaluate the utility of the context network presented in Section 3. We begin by plugging each of the two context modules (Basic and Large) into the front end. Since the receptive field of the context network is 67×67 , we pad the input feature maps by a buffer of width 33. Zero padding and reflection padding yielded similar results in our experiments. The context module accepts feature maps from the front end as input and is given this input during training. Joint training of the context module and the front-end module did not yield a significant improvement in our experiments. The learning rate was set to 10^{-3} . Training was initialized as described in Section 3.

Table 3 shows the effect of plugging the context module on the accuracy of three different architectures for semantic segmentation. The first (top) is the front end described in Section 4, which performs semantic segmentation without structured prediction, akin to the original work of Long et al. (2015). The second (Table 3, middle) uses the dense CRF to perform structured prediction, akin to the system of Chen et al. (2015a). We use the implementation of Krähenbühl & Koltun (2011) and train the CRF parameters by grid search on the validation set. The third architecture (Table 3, bottom) uses the CRF-RNN for structured prediction (Zheng et al., 2015). We use the implementation of Zheng et al. (2015) and train the CRF-RNN in each condition.

The experimental results demonstrate that the context module improves accuracy in each of the three configurations. The basic context module increases accuracy in each configuration. The large context module increases accuracy by a larger margin. The experiments indicate that the context module and structured prediction are synergistic: the context module increases accuracy with or without subsequent structured prediction. Qualitative results are shown in Figure 3.

Evaluation on the test set. We now perform an evaluation on the test set by submitting our results to the Pascal VOC 2012 evaluation server. The results are reported in Table 4. We use the large context module for these experiments. As the results demonstrate, the context module yields a significant boost in accuracy over the front end. The context module alone, without subsequent structured prediction, outperforms DeepLab-CRF-COCO-LargeFOV (Chen et al., 2015a). The context module with the dense CRF, using the original implementation of Krähenbühl & Koltun (2011), performs on par with the very recent CRF-RNN (Zheng et al., 2015). The context module in combination with the CRF-RNN further increases accuracy over the state-of-the-art performance of the CRF-RNN.

We note that concurrently with our work, two groups have achieved even higher accuracy on the VOC-2012 test set by using different structured prediction modules (Lin et al., 2015; Liu et al., 2015). Reference implementations of these systems are not yet available and we were not able to verify whether plugging the context module into these systems boosts accuracy further.

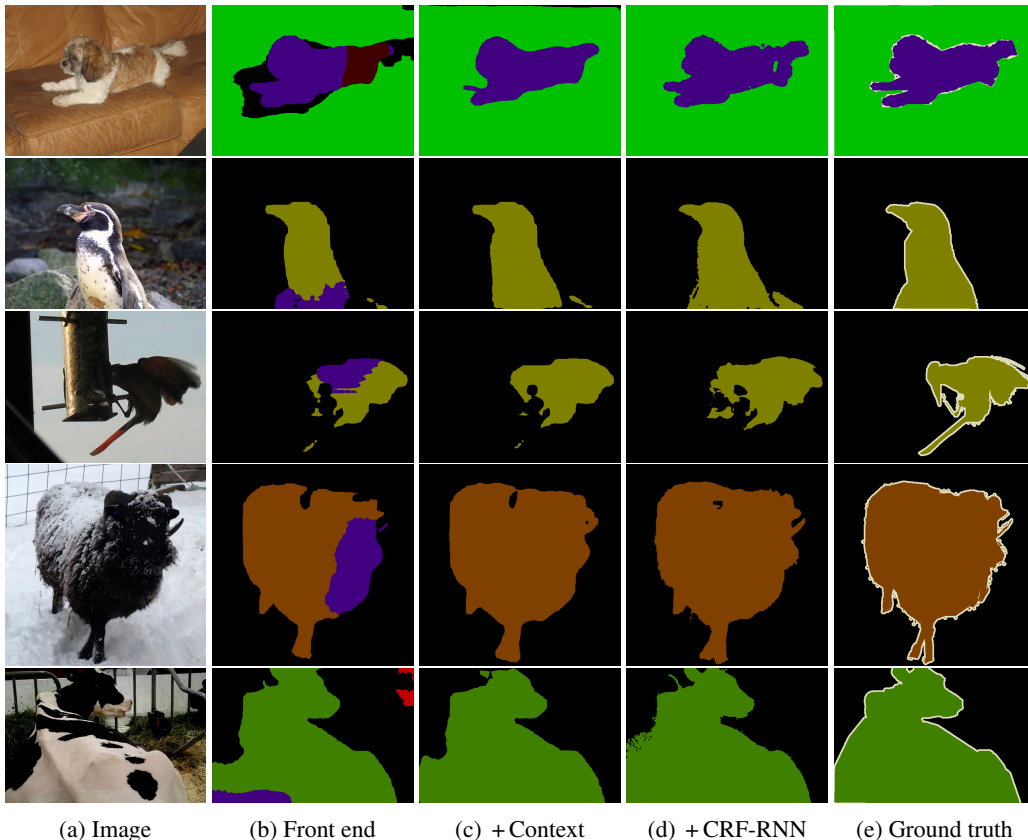


Figure 3: Semantic segmentations produced by different models. From left to right: (a) input image, (b) prediction by the front-end module, (c) prediction by the large context network plugged into the front end, (d) prediction by the front-end + context module + CRF-RNN configuration, (e) ground truth.

	arco	bike	bird	boat	bottle	bus	car	cat	chair	cow	table	dog	horse	mbike	person	plant	sheep	sofa	train	tv	mean IoU
Front end	86.3	38.2	76.8	66.8	63.2	87.3	78.7	82	33.7	76.7	53.5	73.7	76	76.6	83	51.9	77.8	44	79.9	66.3	69.8
Front + Basic	86.4	37.6	78.5	66.3	64.1	89.9	79.9	84.9	36.1	79.4	55.8	77.6	81.6	79	83.1	51.2	81.3	43.7	82.3	65.7	71.3
Front + Large	87.3	39.2	80.3	65.6	66.4	90.2	82.6	85.8	34.8	81.9	51.7	79	84.1	80.9	83.2	51.2	83.2	44.7	83.4	65.6	72.1
Front end + CRF	89.2	38.8	80	69.8	63.2	88.8	80	85.2	33.8	80.6	55.5	77.1	80.8	77.3	84.3	53.1	80.4	45	80.7	67.9	71.6
Front + Basic + CRF	89.1	38.7	81.4	67.4	65	91	81	86.7	37.5	81	57	79.6	83.6	79.9	84.6	52.7	83.3	44.3	82.6	67.2	72.7
Front + Large + CRF	89.6	39.9	82.7	66.7	67.5	91.1	83.3	87.4	36	83.3	52.5	80.7	85.7	81.8	84.4	52.6	84.4	45.3	83.7	66.7	73.3
Front end + RNN	88.8	38.1	80.8	69.1	65.6	89.9	79.6	85.7	36.3	83.6	57.3	77.9	83.2	77	84.6	54.7	82.1	46.9	80.9	66.7	72.5
Front + Basic + RNN	89	38.4	82.3	67.9	65.2	91.5	80.4	87.2	38.4	82.1	57.7	79.9	85	79.6	84.5	53.5	84	45	82.8	66.2	73.1
Front + Large + RNN	89.3	39.2	83.6	67.2	69	92.1	83.1	88	38.4	84.8	55.3	81.2	86.7	81.3	84.3	53.6	84.4	45.8	83.8	67	73.9

Table 3: Controlled evaluation of the effect of the context module on the accuracy of three different architectures for semantic segmentation. Experiments performed on the VOC-2012 validation set. Validation images were not used for training. Top: adding the context module to a semantic segmentation front end with no structured prediction (Long et al., 2015). The basic context module increases accuracy, the large module increases it by a larger margin. Middle: the context module increases accuracy when plugged into a front-end + dense CRF configuration (Chen et al., 2015a). Bottom: the context module increases accuracy when plugged into a front-end + CRF-RNN configuration (Zheng et al., 2015).

6 CONCLUSION

We have examined convolutional network architectures for dense prediction. Since the model must produce high-resolution output, we believe that high-resolution operation throughout the network is both feasible and desirable. Our work shows that the dilated convolution operator is particularly

	areo	bike	bird	boat	bottle	bus	car	cat	chair	cow	table	dog	horse	mbike	person	plant	sheep	sofa	train	tv	mean IoU
DeepLab++	89.1	38.3	88.1	63.3	69.7	87.1	83.1	85	29.3	76.5	56.5	79.8	77.9	85.8	82.4	57.4	84.3	54.9	80.5	64.1	72.7
CRF-RNN	90.4	55.3	88.7	68.4	69.8	88.3	82.4	85.1	32.6	78.5	64.4	79.6	81.9	86.4	81.8	58.6	82.4	53.5	77.4	70.1	74.7
Front end	86.6	37.3	84.9	62.4	67.3	86.2	81.2	82.1	32.6	77.4	58.3	75.9	81	83.6	82.3	54.2	81.5	50.1	77.5	63	71.3
Context	89.1	39.1	86.8	62.6	68.9	88.2	82.6	87.7	33.8	81.2	59.2	81.8	87.2	83.3	83.6	53.6	84.9	53.7	80.5	62.9	73.5
Context + CRF	91.3	39.9	88.9	64.3	69.8	88.9	82.6	89.7	34.7	82.7	59.5	83	88.4	84.2	85	55.3	86.7	54.4	81.9	63.6	74.7
Context + CRF-RNN	91.7	39.6	87.8	63.1	71.8	89.7	82.9	89.8	37.2	84	63	83.3	89	83.8	85.1	56.8	87.6	56	80.2	64.7	75.3

Table 4: Evaluation on the VOC-2012 test set. ‘DeepLab++’ stands for DeepLab-CRF-COCO-LargeFOV (Chen et al., 2015a) and ‘CRF-RNN’ is the system of Zheng et al. (2015). ‘Context’ refers to the large context module plugged into our front end. The context network yields very high accuracy, outperforming the DeepLab++ architecture without performing structured prediction. Combining the context network with the CRF-RNN structured prediction module increases the accuracy of the state-of-the-art CRF-RNN system.

suited to dense prediction due to its ability to expand the receptive field without losing resolution or coverage. We have utilized dilated convolutions to design a new network structure that reliably increases accuracy when plugged into existing semantic segmentation systems. As part of this work, we have also shown that the accuracy of existing convolutional networks for semantic segmentation can be increased by removing vestigial components that had been developed for image classification.

We believe that the presented work is a step towards dedicated architectures for dense prediction that are not constrained by image classification precursors. As new sources of data become available, future architectures may be trained densely end-to-end, removing the need for pre-training on image classification datasets. This may enable architectural simplification and unification. Specifically, end-to-end dense training may enable a fully dense architecture akin to the presented context network to operate at full resolution throughout, accepting the raw image as input and producing dense label assignments at full resolution as output.

State-of-the-art systems for semantic segmentation leave significant room for future advances. Failure cases of our most accurate configuration are shown in Figure 4. We will release our code and trained models to support progress in this area.

REFERENCES

- Chen, Liang-Chieh, Papandreou, George, Kokkinos, Iasonas, Murphy, Kevin, and Yuille, Alan L. Semantic image segmentation with deep convolutional nets and fully connected CRFs. In *ICLR*, 2015a.
- Chen, Liang-Chieh, Yang, Yi, Wang, Jiang, Xu, Wei, and Yuille, Alan L. Attention to scale: Scale-aware semantic image segmentation. *arXiv:1511.03339*, 2015b.
- Everingham, Mark, Gool, Luc J. Van, Williams, Christopher K. I., Winn, John M., and Zisserman, Andrew. The Pascal visual object classes (VOC) challenge. *IJCV*, 88(2), 2010.
- Farabet, Clément, Couprie, Camille, Najman, Laurent, and LeCun, Yann. Learning hierarchical features for scene labeling. *PAMI*, 35(8), 2013.

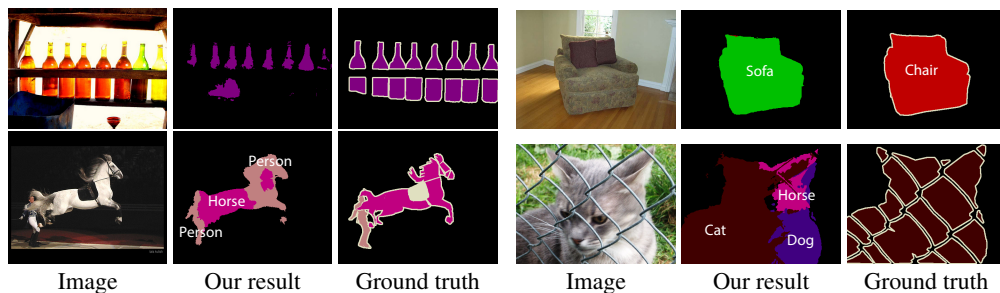


Figure 4: Failure cases from the VOC-2012 validation set. The most accurate architecture we trained (Context + CRF-RNN) performs poorly on these images.

- Fischer, Philipp, Dosovitskiy, Alexey, Ilg, Eddy, Häusser, Philip, Hazrba, Caner, Golkov, Vladimir, van der Smagt, Patrick, Cremers, Daniel, and Brox, Thomas. Learning optical flow with convolutional neural networks. In *ICCV*, 2015.
- Galleuillos, Carolina and Belongie, Serge J. Context based object categorization: A critical survey. *Computer Vision and Image Understanding*, 114(6), 2010.
- Glorot, Xavier and Bengio, Yoshua. Understanding the difficulty of training deep feedforward neural networks. In *AISTATS*, 2010.
- Hariharan, Bharath, Arbelaez, Pablo, Bourdev, Lubomir D., Maji, Subhansu, and Malik, Jitendra. Semantic contours from inverse detectors. In *ICCV*, 2011.
- He, Xuming, Zemel, Richard S., and Carreira-Perpiñán, Miguel Á. Multiscale conditional random fields for image labeling. In *CVPR*, 2004.
- Holschneider, M., Kronland-Martinet, R., Morlet, J., and Tchamitchian, Ph. A real-time algorithm for signal analysis with the help of the wavelet transform. In *Wavelets: Time-Frequency Methods and Phase Space. Proceedings of the International Conference*, 1987.
- Jia, Yangqing, Shelhamer, Evan, Donahue, Jeff, Karayev, Sergey, Long, Jonathan, Girshick, Ross B., Guadarrama, Sergio, and Darrell, Trevor. Caffe: Convolutional architecture for fast feature embedding. In *Proc. ACM Multimedia*, 2014.
- Kohli, Pushmeet, Ladicky, Lubor, and Torr, Philip H. S. Robust higher order potentials for enforcing label consistency. *IJCV*, 82(3), 2009.
- Krähenbühl, Philipp and Koltun, Vladlen. Efficient inference in fully connected CRFs with Gaussian edge potentials. In *NIPS*, 2011.
- Krizhevsky, Alex, Sutskever, Ilya, and Hinton, Geoffrey E. ImageNet classification with deep convolutional neural networks. In *NIPS*, 2012.
- Le, Quoc V., Jaitly, Navdeep, and Hinton, Geoffrey E. A simple way to initialize recurrent networks of rectified linear units. *arXiv:1504.00941*, 2015.
- LeCun, Yann, Boser, Bernhard, Denker, John S., Henderson, Donnie, Howard, Richard E., Hubbard, Wayne, and Jackel, Lawrence D. Backpropagation applied to handwritten zip code recognition. *Neural Computation*, 1(4), 1989.
- Lin, Guosheng, Shen, Chunhua, Reid, Ian, and van den Hengel, Anton. Efficient piecewise training of deep structured models for semantic segmentation. *arXiv:1504.01013*, 2015.
- Lin, Tsung-Yi, Maire, Michael, Belongie, Serge, Hays, James, Perona, Pietro, Ramanan, Deva, Dollár, Piotr, and Zitnick, C. Lawrence. Microsoft COCO: Common objects in context. In *ECCV*, 2014.
- Liu, Ziwei, Li, Xiaoxiao, Luo, Ping, Loy, Chen-Change, and Tang, Xiaoou. Semantic image labeling via deep parsing network. In *ICCV*, 2015.
- Long, Jonathan, Shelhamer, Evan, and Darrell, Trevor. Fully convolutional networks for semantic segmentation. In *CVPR*, 2015.
- Noh, Hyeonwoo, Hong, Seunghoon, and Han, Bohyung. Learning deconvolution network for semantic segmentation. In *ICCV*, 2015.
- Rumelhart, David E., Hinton, Geoffrey E., and Williams, Ronald J. Learning representations by back-propagating errors. *Nature*, 323, 1986.
- Shensa, Mark J. The discrete wavelet transform: wedding the à trous and Mallat algorithms. *IEEE Transactions on Signal Processing*, 40(10), 1992.
- Shotton, Jamie, Winn, John M., Rother, Carsten, and Criminisi, Antonio. TextonBoost for image understanding: Multi-class object recognition and segmentation by jointly modeling texture, layout, and context. *IJCV*, 81(1), 2009.
- Simonyan, Karen and Zisserman, Andrew. Very deep convolutional networks for large-scale image recognition. In *ICLR*, 2015.
- Zheng, Shuai, Jayasumana, Sadeep, Romera-Paredes, Bernardino, Vineet, Vibhav, Su, Zhizhong, Du, Dalong, Huang, Chang, and Torr, Philip. Conditional random fields as recurrent neural networks. In *ICCV*, 2015.